



Barsukov Yuri Vladimirovich

Plasma processes affecting etching and growth of nitride materials

01.04.08 – plasma physics

ABSTRACT

of thesis for the PhD degree

Saint-Petersburg

2022

Thesis is done in Peter the Great Saint-Petersburg State University

Scientific supervisor is Prof. Alexander Sergeevich Smirnov

Official opponents:

Dr. Timofeev Nickolay Alexandrovich

Dr. Schweigert Irina Vacheslalovna

Prof. Saint-Petersburg State University

Senior Researcher, Khristianovich
Institute of Theoretical and Applied
Mechanics

Externa Reviewer Petersburg Nuclear Physics Institute

Thesis Defense will be held on April 18 2022

at a meeting of the Dissertation Committee Y.01.04.08

of Peter the Great St. Petersburg Polytechnic University.

(195251, Russia, St.Petersburg, Polytechnicheskaya, 29, building 2, room 425).

Thesis can be found in the library

and on website https://www.spbstu.ru/science/the-department-of-doctoral-studies/defences-calendar/the-degree-of-candidate-of-sciences/barsukov_yuriy_vladimirovich/

of Peter the Great St. Petersburg Polytechnic University.

The abstract is sent on _____

date

Scientific Secretary of the Dissertation Committee

Dr. Kaveeva Elisaveta Genadievna



Introduction

Relevance of the work

Plasma treatment is widely used in semiconductor industry during integrated circumstance fabrication. Particular, a dry isotropic etching is one of the most challenge step during FEOL (front end of line) step of nanofabrication of integrated circumstance based on CMOS technology (complementary metal oxide semiconductor) [1]. The dry etching implies interaction of the surface with neutral species, and the last ones are generated in a remote plasma source (RPS). Damage free etcher with RPS is typically used for such kind of etching, where plasma has no contact with the etched surface in order to exclude the surface damage by UV emission and ion bombardments. A sandwich-like structure with silicon oxide (SiO_2) and silicon nitride (Si_3N_4) layers is formed during one of step of 3D-NAND memory fabrication. At the next step, the Si_3N_4 layer is horizontally removed forming a cavities, which are in turn filled by wolfram (metallization step) [2]. A wet etching using hot phosphoric acid is used so far to remove silicon nitride with high selectivity over silicon oxide [3,4]. The $\text{Si}_3\text{N}_4/\text{SiO}_2$ selectivity is $\text{ER}(\text{Si}_3\text{N}_4)/\text{ER}(\text{SiO}_2)$ ratio, where ER is etch rate. Plasma etching is very promising technology. In future, it should fully replace wet etching in the semiconductor industry. Thus, to study a process of highly selective etching of Si_3N_4 by remote plasma source is relevance task for the industry.

Another important application of plasma is synthesis of new materials. For example, boron nitride BN is isoelectronic analogous of carbon, and BN is able to form similar structures as carbon [5]: fullborenes (0D), nanotubes (1D), hexagonal graphite sheets (2D), diamond like crystals (3D). The most of these structures cannot be found in nature, therefore they are produced by synthesis. Due to polarity of the B-N bond (C-C is nonpolar bond), BN compounds have unique properties. For example, BN structures are resistant to chemical attack [6] and to heating [7]. Moreover, defect free BN nanostructures have a wide band gap [8], therefore they can be used in optoelectronics [9]. BN nanotubes (BNNT) were synthesis in the labs using high temperatures synthesis. Namely, arc discharge [10,11] and ICP (inductively coupled plasma) torch [12–14] were used during the synthesis. Despite this fact, this is still no technology for a large-scale production of BNNTs. One of the main impediment to large scale production is liquid boron consumption during the synthesis. Thus, to study a process of BNNT synthesis and determine a key process of this synthesis is relevance task for the modern industry.

Objectives and targets

The main objective of my research is to determine an optimal conditions of gas discharges to plasma etching of silicon nitride (with high selectivity relevant to silicon oxide) and to large scale

production of boron nitride nanotubes with high purity. It was suggested to determine chemical reagents to etch silicon nitride, while no silicon oxide etching. These reactants are in turn generated in the remote source of NF_3/O_2 and $\text{NF}_3/\text{O}_2/\text{N}_2/\text{H}_2$ plasmas. In addition, to study a mechanism of N_2 molecule fixation process and a precursor formation of boron nitride nanotube growth during a high temperature synthesis, and to determine key factors, which affect on the boron consumption.

It was suggested and solved the following targets:

1. Conducting of experiments towards to study a highly $\text{Si}_3\text{N}_4/\text{SiO}_2$ selective etching using remote source of NF_3/O_2 and $\text{NF}_3/\text{O}_2/\text{N}_2/\text{H}_2$ plasmas.
2. Using quantum chemistry methods to develop a mechanism of Si_3N_4 etching, determine key reagents for the selective etching, calculate rate constant of surface reactions leading to etching.
3. Based on the suggested mechanism to develop an analytical mode of the etching, which will describe a dependence of the etch rates of silicon oxide and nitride on the fluxes of reactants.
4. To make a comparison between results of analytical modelling and experimental data and prove a correctness of the model. Also, a model of NF_3/O_2 and $\text{NF}_3/\text{O}_2/\text{N}_2/\text{H}_2$ plasmas will be developed. In addition, densities of radicals and molecules will be measured by actinometry and mass-spectrometry.
5. To determine key reagents for the high $\text{Si}_3\text{N}_4/\text{SiO}_2$ selective etching based on the modelling and experimental data.
6. To calculate the thermodynamic potentials (Gibbs free energy) for B-N compounds. These potentials will be used to determine a composition of B/ N_2 mixture at thermodynamic equilibrium using Gibbs free energy minimization method.
7. To make a modelling of the reactions between N_2 molecules and small boron clusters in gas phase and calculate rate constants of these reactions, where B-N compounds are generated (N_2 fixation).
8. To develop a kinetic system of equation. This system of equation will describe the process of N_2 fixation and formation of B-N compounds. The last ones are the precursors of boron nitride nanotube growth in the cooling gas mixture.

Novelty

1. It was shown that the key reagent of the etching by NF_3/O_2 plasma are NO (nitric oxide) and F atom. Note, that NO enhance the etching of Si_3N_4 , while no effect on the SiO_2 etching. Atomic fluorine etches both silicon oxide and silicon nitride, therefore the selectivity is not high for such kind of etching.

2. A mechanism of Si₃N₄ etching by F atoms and NO was developed based on the results of quantum chemistry modelling. According to the suggested mechanism, new N-F bonds caused by the subsequent reaction steps are formed during the etching: $F + \sim Si-N-Si \sim = \sim Si-F + \cdot N-Si \sim$; $F + \cdot N-Si \sim = F-N-Si \sim$. Then, NO reacts with F-N bonds of the fluorinated surface resulting in enhancing migration of F atoms from the N surface atom on the neighboring Si surface atom: $NO + F-N-Si \sim = N_2O + F-Si \sim$. As a result, the volatile by-products of the etching are generated, such as SiF₄ и N₂O, and the etch rate increases. Suggested analytical model quantitatively describes the dependence of the silicon nitride and oxide etch rates on the fluxes of F atoms and NO.

3. By analogous with NO, the quantum chemistry modelling was performed to study the reactions between HF, Cl, H, Br и FNO species with F-N surface bond. According to the modelling data, these species accelerate the migration of surface F atoms also. This result is able to quantitatively explain the early published experimental data.

4. For the first time, it was that the curve of Si₃N₄/SiO₂ selectivity in dependence of H₂ flow rate in the afterglow area of NF₃/O₂/N₂ plasma has a high and narrow peak. Namely, the selective peak is near the point, where density of F atoms equals to density of H₂ ($[F] \approx [H_2]$).

5. It was shown that the density of the vibrational excited species HF(v) has a peak near the $[F] \approx [H_2]$ point.

6. It was developed a mechanism and analytical model of the Si₃N₄ and SiO₂ etching by NF₃/O₂/N₂/H₂ remote plasma. According to the suggested model, the main etchants of both silicon oxide and nitride are F atoms and HF molecule in ground and vibrationally excited states. At room temperature, HF molecule at the ground state is able to etch Si₃N₄ and SiO₂ in the presence of catalysts. Particular, water molecules play a role of the catalyst in the downstream plasma. Thus, the suggested analytical model describes the dependence of Si₃N₄ and SiO₂ etch rate on the fluxes of F, HF(v=0), HF(v=1) и H₂O.

7. Based the comparison of the modelling data with the experimental data, it was shown for the first time that vibrationally excited HF(v) molecules are able to initiate the etching of Si₃N₄, while no SiO₂ etching. As a result, the Si₃N₄/SiO₂ selectivity of this etching is very high.

8. For the first time, it was experimentally shown a kinetic isotope effect on the reactive ion etching of Si₃N₄: the etch rate drops by replacing H₂ with D₂ in SF₆/H₂ plasma.

9. For the first time, it was suggested a mechanism of N₂ fixation process resulting in formation of B-N compounds, which are in turn precursors of the boron nitride nanotubes growth during the high temperature synthesis. It was theoretically shown that dissociative adsorption of N₂ molecules on small boron clusters (B_m) occurs at the temperatures below boron condensation point. Eventually $n/2N_2 + B_m$ results to formation of B_mN_n linear chains (with $n \leq 12$, $m = n+1$ or n).

Moreover, these B_mN_n linear chains are the main components of the reaction mixture at the thermodynamic equilibrium at the temperature range from 2600 to 3000K at 1 atm pressure.

10. It was shown that the process of N_2 fixation is the rate-limiting step, which determines the boron consumption in B/ N_2 mixture. The boron consumption increases at high pressure and low initial boron fraction in the mixture. That make a good condition to large scale production of high-quality and purity boron nitride nanotubes.

Practical and scientific value

1. For the first time, it was shown that vibrationally excited molecules $HF(v)$ initiate the highly selective etching of silicon nitride without catalyst.

2. It was suggested new reagents which are able to enhance the Si_3N_4 etching in the presence of F atoms, such as HF, Cl, H, Br и FNO. Moreover, these reagents should stronger enhance the etching of silicon nitride than NO.

3. For the first time, it was shown that the dissociative adsorption of N_2 on small boron clusters (N_2 fixation process) determine the boron consumption during high temperature synthesis. In addition, the system does not achieve an equilibrium during the gas cooling at a typical for the synthesis gas cooling rates. It was shown that fixation of N_2 increases at high pressure, low initial boron fraction and low gas cooling rate resulting in high boron consumption.

4. It was shown for the first time that B-N linear chains and monocyclic rings are the most stable B-N compounds at the narrow temperature range (~2600-3000K at 1 atm pressure).

Thesis Statements

1. The etch rate of the silicon nitride by the NF_3/O_2 remote plasma is a function of the fluxes of F atoms and NO radicals. Atomic fluorine fluorinates and etches the surface, while nitric oxide enhances the etching interacting with the fluorinated surface. A role of NO in the etching of silicon nitride by NF_3/O_2 remote plasma appears in the presence of F atoms only, therefore the Si_3N_4/SiO_2 selectivity is limited due to the F atom presence.

2. Highly Si_3N_4/SiO_2 selective etching by $NF_3/O_2/N_2/H_2$ remote plasma occurs near the point, where density of F atoms equals to density of H_2 molecules $[F] \approx [H_2]$. The key reagents of such kind of etching are F atom, $HF(v=0)$, $HF(v=1)$ and H_2O .

3. Vibrationally excited molecules $HF(v)$ is able to initiate the highly Si_3N_4/SiO_2 selective etching of without a catalyst.

4. The process of N_2 fixation during high temperature synthesis of boron nitride nanotubes determines the rate of boron consumption. Fixation of N_2 molecule fixation occurs through the reactions between N_2 molecules and small B_m clusters.

5. The processes of N₂ fixation and boron consumption occurs at non-equilibrium regime at a typical gas cooling rate during high temperature synthesis.

6. The boron consumption during high temperature synthesis of boron nitride nanotubes increases at high pressure, low gas cooling rate and low initial boron fractions. s

7. B-N linear chains and monocyclic rings are thermodynamically the most stable compounds in B/N₂ mixture at narrow temperature range: higher the temperature suitable for the boron nitride nanotubes growth (~ 2400 K) and below boron condensation point.

Validity of the results

It was used the modern setups during this research. All results were reproduced. All results are in agreement with the theoretical model, do not contradict to the published data. All results were tested on the Russian and international conferences.

Test of the research

The results of my thesis were many times discussed reported on the seminars in the Department of Physics of Optics of Saint-Petersburg State University, Department of Quantum Chemistry of Saint-Petersburg State University, Quantum Chemistry Lab in Petersburg Institute of Nuclear Physics, Plasma Physic Department of Peter the Great Saint-Petersburg Polytechnic University, Lab of Plasma Physics and Basis of Microtechnology, “Coddan Technology” Ltd. (Russia, SPb), “Corial” company (Grenoble, France), LLC “Samsung Electronics” (South Korea), Princeton Plasma Physics Lab (USA), Applied Materials Inc. (California, USA).

This research was presented on five conferences:

- 24th International Symposium on Plasma Chemistry (Naples (Italy), June 9-14 2019)
- Nature – “Advances and Applications in Plasma Physics” (Saint-Petersburg (Russia), September 18-20 2019).
- International Conference PhysicA.SPb Saint-Petersburg (Russia), 2020.
- The 73rd Annual Gaseous Electronics Conference (virtual), 2020
- 63rd Annual Meeting of the APS Division of Plasma Physics (virtual), 2020

My Publications

[1] Yu. Barsukov, V. Volynets, S. Lee, G. Kim, B. Lee, S.K. Nam, and K. Han. Role of NO in highly selective SiN/SiO₂ and SiN/Si etching with NF₃/O₂ remote plasma: Experiment and simulation // J. Vac. Sci. Technol. A. 2017, V. 35, P. 061310. DOI: 10.1116/1.5004546.

[2] Yu.V. Barsukov, V. Volynets, A.A. Kobelev, N.A. Andrianov, A.V. Tulub, and A.S. Smirnov. Enhanced silicon nitride etching in the presence of F atoms: Quantum chemistry simulation // J. Vac. Sci. Technol. A. 2018, V. 36, P. 061301. DOI: 10.1116/1.5044647.

[3] V. Volynets, V. Protopopov, Y.D. Kim, Yu. Barsukov, S.H. Lee, and S.H. Jang. Pulsed plasma analyzer and method for analyzing the same // US Patent. 2018, 0130651 A1.

[4] G.J. Kim, Yu. Barsukov, V. Volynets, D. Liu, S.J. An, B.J. Lee, and S. Patel. Etching method using remote plasma source, and method of fabricating semiconductor device including the etching method // US Patent. 2018, 0374709 A1.

[5] P. Pankratiev, Yu. Barsukov, A. Vinogradov, V. Volynets, A. Kobelev, A.S. Smirnov. Selective SiN/SiO₂ etching by SF₆/H₂/Ar/He Plasma // AIP Conf. Proc. 2179. 2019, P. 020017. DOI: 10.1063/1.5135490.

[6] V. Volynets, Yu. Barsukov, G.J. Kim, J.E. Jung, S.K. Nam, K. Han, S. Huang, and M.J. Kushner. Highly selective Si₃N₄/SiO₂ etching using an NF₃/N₂/O₂/H₂ remote plasma. I. Plasma source and critical fluxes // J. Vac. Sci. Technol. A. 2020, V. 38, P. 023007. DOI: 10.1116/1.5125568.

[7] J.E. Jung, Yu. Barsukov, V. Volynets, G. Kim, S.K. Nam, K. Han, S. Huang, and M.J. Kushner. Highly selective Si₃N₄/SiO₂ etching using an NF₃/N₂/O₂/H₂ remote plasma. II. Surface reaction mechanism // J. Vac. Sci. Technol. A. 2020, V. 38, P. 023008. DOI: 10.1116/1.5125569.

[8] P.A. Pankratiev, Yu.V. Barsukov, A.A. Kobelev, A.Ya. Vinogradov, I.V. Miroshnikov, and A.S. Smirnov. Etching of Si₃N₄ by SF₆/H₂ and SF₆/D₂ plasmas // J Phys.: Conf. Ser. 2020, V. 1697, P. 012222. DOI: 10.1088/1742-6596/1697/1/012222.

[9] Yu. Barsukov, O. Dwivedi, I. Kaganovich, S. Jubin, A. Khrabry, and S. Ethier. Boron nitride nanotube precursor formation during high-temperature synthesis: kinetic and thermodynamic modelling // Nanotechnology, 2021, V. 32, P. 475604. DOI: 10.1088/1361-6528/ac1c20.

Personal Contribution

All presented here results were obtained by myself or with my participation. I give significant contribution in all presented here experimental measurements, treatment of the data, quantum chemistry modelling, development of the chemical mechanisms and analytical modelling.

All results of my research presented here were obtained in Samsung Electronics Ltd. and Peter the Great Saint-Petersburg Polytechnic University.

Table of content

Novelty, objectives and targets of this research as well as list of my publications and conferences were considered in the **Introduction**.

Literature review is presented in the **First Section**. It is considered mechanisms of the etching of silicon-based materials. Such as silicon nitride, silicon oxide and doped and undoped silicon. It is considered the etching of silicon nitride by remote NF_3/O_2 and CF_4/O_2 plasmas, as well as a role of NO in this etching. The mechanisms of silicon nitride and oxide by HF molecule with H_2O and NH_3 catalyst were considered. The literature review of high temperature synthesis of BNNT can be found in this section also.

The result of my research aimed to study of $\text{Si}_3\text{N}_4/\text{SiO}_2$ selective etching by NF_3/O_2 remote plasma is presented in **Section 2**. The experimental setup (DFE or damage free etcher) with ICP remote plasma source (RPS) is described. This setup was made in Samsung Electronics Ltd.

Optical spectra were measured in the range between 200 nm and 800 nm. Actinometry method [15–17] was used to measure the densities of F and O atoms, therefore small amount of Ar was injected in the plasma zone. Due to the fact, only limited amount of species can be measured a plasma modelling was performed using Global Kin code [18,19]. The measured and calculated densities of F atoms and NO radicals are presented in Fig. 1.

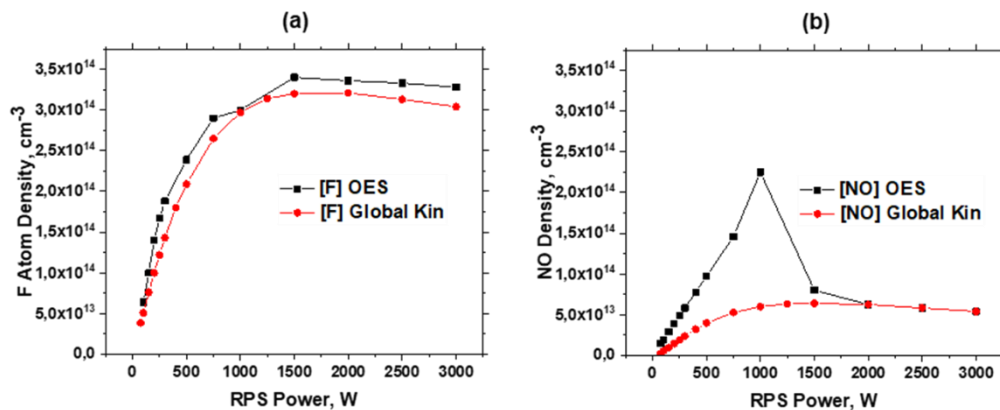


Fig 1. Dependence of concentrations [F] (a) u [NO] (b) on plasma power.

The calculation very accurately reproduces the density of F atoms as opposite to NO. Moreover, the calculation showed the monotonic growth of the NO density with plasma power, while measured emission of NO radical has a peak near 1000 W power. Note, the measured density of NO was used in the analytical modelling.

Table 1. List of reaction, which were considered in the model of Si_3N_4 etching by F and NO.

R_i	Поверхностная реакция	γ_i
R1	$\text{F} + \theta 1 \rightarrow \text{SiF}_4 + \theta 2$	1.5×10^{-3}
R2	$\text{F} + \theta 2 \rightarrow \theta 3$	1.0
R3	$\text{F} + \theta 3 + \text{bulk} \rightarrow \text{SiF}_4 + \text{N}_2 + \theta 1$	1.2×10^{-4}
R4	$\text{NO} + \theta 3 + \text{bulk} \rightarrow \text{SiF}_4 + \text{N}_2\text{O} + \theta 1$	1.8×10^{-4}

Based on quantum chemistry calculations, the mechanism of Si_3N_4 etching by F atoms and NO were suggested. According to this mechanism, NO radicals promote the migration of F atoms from the surface N atoms on the neighboring Si atoms. In other words, NO decreases the barrier of this migration resulting in enhanced silicon nitride etching.

The analytical model of Si_3N_4 and SiO_2 etching were suggested. This model described the dependence of the etch rates on the fluxes of F and NO.

The result of analytical model as well as experimental data are presented in Fig. 2. That model implies zero etch rate in the absence of atomic fluorine. In other words, NO can enhance the etching, NO cannot etch without atomic fluorine.

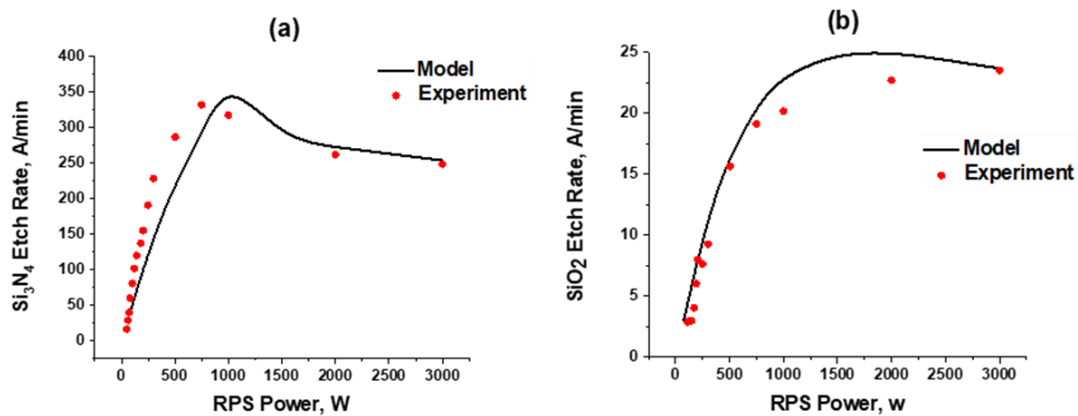


Рисунок 2. Calculated and measured etch rates of silicon nitride (a) and oxide (b) in dependence of the NF_3/O_2 plasma power.

It is known from previous publications [20] that NO enhances the etching of silicon nitride. According to the suggested here mechanism of the etching F atom breaks Si-N bond resulting in formation of new Si-F bond and free bond on the N atom. This free bond is closed by the second F atom resulting in F-N bond formation. Then, NO reacts with the F-N bond and, as a result, F atom migrate from F-N bond on the neighboring Si atom and N_2O molecule is formed. Note, eventually the final products of these reaction are volatile by-products, such as SiF_4 , N_2 и N_2O .

These by-products were experimentally detected during the etching of silicon nitride [21]. Thus, atomic fluorine is essential for such kind of etching, therefore $\text{Si}_3\text{N}_4/\text{SiO}_2$ is limited.

Section 3 is aimed to quantum chemistry modelling of the F atom migration from the F-N in $\text{SiF}_3\text{-NF-SiF}_2\text{-NF-SiF}_3$ cluster under treatment by NO, HF, Cl, H, Br and FNO. According to the suggested mechanism, this migration is a rate-limiting step of the etching. It was shown that NO, HF, Cl, H, Br и FNO accelerates of the migration. Moreover, HF, Cl, H, Br и FNO accelerate faster this migration than NO. This fact is able to quantitatively explain some published experimental data. As it was mentioned above the presence of F atoms significantly lowers the $\text{Si}_3\text{N}_4/\text{SiO}_2$ selectivity, therefore it was suggested to add H_2 in the NF_3/O_2 mixture. Gradual addition of H_2 decreases density of F atoms through $\text{F} + \text{H}_2 \rightarrow \text{HF} + \text{H}$ reaction resulting in high $\text{Si}_3\text{N}_4/\text{SiO}_2$ selectivity.

Section 3 is aimed to study highly selective $\text{Si}_3\text{N}_4/\text{SiO}_2$ etching by $\text{NF}_3/\text{O}_2/\text{N}_2/\text{H}_2$ plasma. It was shown that $\text{Si}_3\text{N}_4/\text{SiO}_2$ selectivity dramatically increases near the point, where $[\text{F}] \approx [\text{H}_2]$. Note, that the densities of atomic fluorine and H_2 molecule are coupled by the following reaction

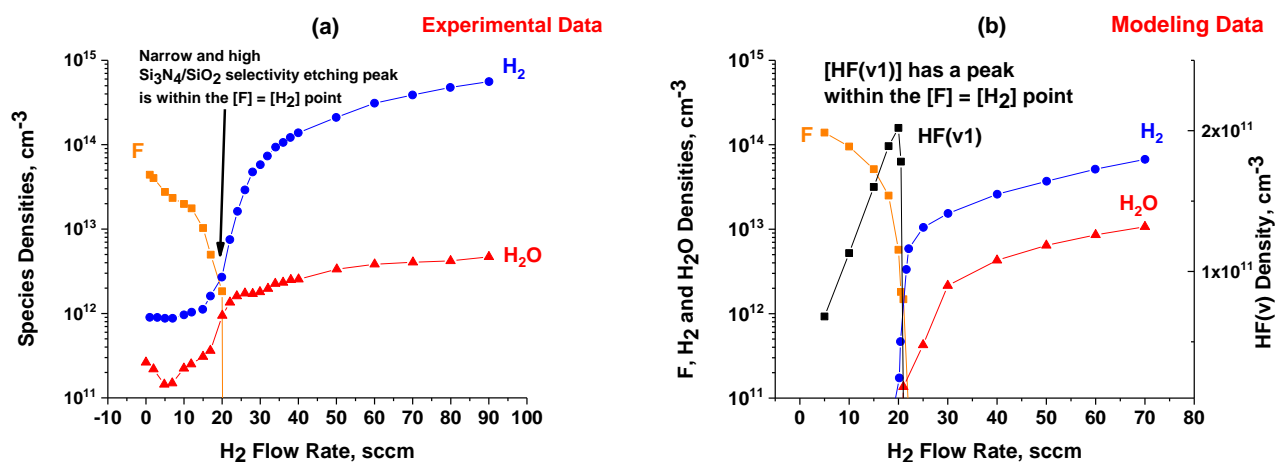


Рисунок 3. Measured (a) and calculated (b) densities $[\text{F}]$, $[\text{H}_2]$, $[\text{H}_2\text{O}]$ and $[\text{HF}(\text{v}1)]$ in the process chamber in dependence on H_2 flow rate.

Densities of F and H_2 were measured using actinometry and mass-spectrometry methods. As it is shown in Fig. 3a both F and H_2 densities ($[\text{F}]$ and $[\text{H}_2]$) strongly depends on H_2 flow rate. At low H_2 flow rate the density of F atoms monotonically decreases with H_2 flow rate increasing. The decline of F atom density becomes stronger at H_2 flow rate higher than 20 sccm. Then $[\text{F}]$ achieves a plateau at H_2 flow rate in the range 22 - 90 sccm. The density of H_2 , which was measured using mass-spectrometry, has the different trend. Indeed, at low H_2 flow rate (0 - 20 sccm) the density of H_2 slowly increases, then this growth dramatically accelerates at the ~ 20 sccm H_2 flow rate.

Sharp decline of [F] and sharp growth of [H₂] occurs near the [F]≈[H₂] point. Optical spectrum was measured in the 200 nm – 800 nm range, which does not cover HF(v) emission (2.5 μm). Therefore, [HF(v1)] was calculated using plasma modelling code. As it is shown in Fig. 3b, the densities of atomic fluorine, molecular hydrogen and water agreed with the measured densities well. Note, the density of HF(v1) molecular at first vibration excitation has a high peak in the same area (it is near the [F]≈[H₂] point), where Si₃N₄/SiO₂ selectivity has a high and narrow peak. According to the modelling data, the density of HF(v2) is near $2 \times 10^{11} \text{ cm}^{-3}$. According to the analytical modelling, this density number is enough to support the etch rate of Si₃N₄ on a significant level near the [F]≈[H₂] point. At the same time, SiO₂ etch rate has a minimum value near the [F]≈[H₂] point, because the densities of both F and H₂O are very low near this point. Indeed, it is known that H₂O catalyzes the SiO₂ etching by HF molecule at the ground state. It is known, that dry HF gas in the absence of water vapors begins to etch SiO₂ at T>1000 K [22]. Water is catalysis of the etching [23] and the presence of water is essential for the etching by HF. In other words, near the [F]≈[H₂] point SiO₂ etch rate has a minimum value as opposite to Si₃N₄ etch rate, because Si₃N₄ is etched by vibrationally excited HF(v) molecules.

The surface reactions which were used in the analytical model of the etching is shown in Table 2. The following surface sites were introduced: θ_1 – initial surface site of Si₃N₄ or SiO₂, θ_2 – surface sites with adsorbed HF molecule at the ground state HF(v=0), θ_3 – surface site with two adsorbed HF molecules HF(v0) + HF(vs1) one of which is vibrationally excited molecule, θ_4 – surface site with HF molecule at the ground state and water molecule HF(v=0) + H₂O.

We assumed that the etching occurs at the steady state conditions and the surface composition is not a function of time. Moreover, we assumed that the surface reactions do not significantly change the fluxes of the reactant near the surface. Molecules of HF(v0), HF(v1) and H₂O, which are generate in the downstream plasma, are adsorbed on the θ_1 surface sites resulting in formation of θ_2 , θ_3 или θ_4 sites (R1, R2 and R5 reactions in Table 2). Desorption of these species from the surface leads to the formation of θ_1 sites (R3 and R4 reactions in Table 2). Reactions of the etching leads to formation of volatile by-products (SiF₄, NH₃, HF and H₂O), which is denoted as EP or etch products (R6, R7 and R8 reactions). Only HF(v1) molecules at the first vibrational excitation was taking into account. These vibrationally excited HF(v1) molecules are adsorbed on θ_2 sites (R2 reaction), and the etching occurs through R7 reaction.

Table 2. List of the reactions and rate constants, which was used in the analytical of Si₃N₄ and SiO₂ etching by F, HF, H₂O u HF(v1).

	Поверхностные реакции	γ		A (1/s)		E _a /R (K)	
		Si ₃ N ₄	SiO ₂	Si ₃ N ₄	SiO ₂	Si ₃ N ₄	SiO ₂
R1	HF + $\theta_1 \rightarrow \theta_2$	1	1	-	-	-	-
R2	HF(v=1) + $\theta_2 \rightarrow \theta_3$	1	1	-	-	-	-
R3	$\theta_2 \rightarrow$ HF + θ_1	-	-	5.00×10^7	9.00×10^9	2044	1996
R4	$\theta_3 \rightarrow$ 2HF + θ_1	-	-	2.10×10^9	8.00×10^{10}	3612	0
R5	H ₂ O + $\theta_2 \rightarrow \theta_4$	1	1	-	-	-	-
R6	$\theta_4 \rightarrow$ EP + θ_1	-	-	1.18×10^{10}	1.46×10^{13}	7862	7399
R7	$\theta_3 \rightarrow$ EP + θ_1	-	-	4.02×10^{11}	6.55×10^8	1756	8061
R8	F + $\theta_1 \rightarrow$ EP + θ_1	0.00001	0.0000195	-	-	-	-

The rate constant of R3, R4, R6 и R7 reactions are in Arrhenius form:

$$k_i = A_i \exp\left(-\frac{E_{ai}}{RT}\right). \quad (3)$$

Activation energies (E_a) were calculated as an energy difference between reactant complex and transition state. Transition state theory [24] and Eyring equation [25] were used to calculate a pre-exponential factors A_i for R6 и R7 reactions,

$$A_i = \frac{k_B T}{h} \times \left(\frac{Z_{vib}^{TS}}{Z_{vib}^{Re}}\right), \quad (4)$$

where k_B и h are Boltzmann and Planck constants, Z_{vib}^{TS} and Z_{vib}^{Re} – vibrational partition functions of transition start and reactant complex, respectively. The partition functions were calculated using Gaussian 09 software package [26].

Reagents in the R6 and R7 reactions are adsorbed molecules: HF + H₂O и HF + HF(v1). Molecule of HF reacts with both Si₃N₄ and SiO₂ at room temperature only in the presence of the catalyst (water in our case). Internal vibrational energy of HF(v1) molecule is used to overcome the barrier of the surface reaction leading to the etching of Si₃N₄. It is known that the vibrational quantum energy of O-H and F-H bonds are very close to each other, therefore HF(v1) should be quasi-resonantly quenched in a collision with hydroxyl groups of oxide surface. Thus, the residence time of the vibrationally excited HF(v) molecules is a function of the average time of the etching reactions and quenching. Due to the fact that the transition of vibrational quantum from

HF(v) molecule on the hydroxyl groups is quasi-resonance process, molecules of HF(v1) are quenched on the oxide surface without etching.

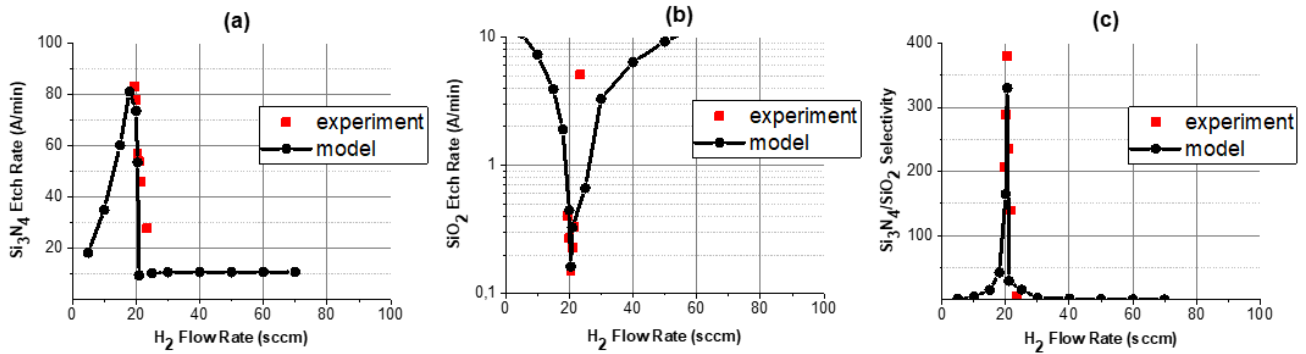


Figure 4. Measured and calculated etch rates of Si₃N₄ and SiO₂ as well as Si₃N₄/SiO₂ selectivity in dependence of H₂ flow rate: (a) etch rate of Si₃N₄, (b) etch rate of SiO₂ and (c) Si₃N₄/SiO₂ selectivity.

The data of the etching and the selectivity data, which were calculated using the analytical model of the etching as well as experimental data, are presented in Fig. 4. The calculated data correlate with the experimental data well. The etch rate of Si₃N₄ and Si₃N₄/SiO₂ selectivity peaks near 20 sccm H₂.

The contribution of F, HF + H₂O and HF + HF(v1) to the total etch rate of Si₃N₄ and SiO₂ in dependence of H₂ flow rate is shown in Fig. 5. The etch rate by F atoms decreases with H₂ flow rate, because the density of F decreases with H₂ flow rate. The contribution of HF(v1) to the etching of Si₃N₄ is determined by the flux of HF(v1). The flux of HF(v1) peaks near the [F]≈[H₂] point. The water production is slow at [H₂]<[F], and it dramatically increases at [H₂]>[F]. As a result, the etching by HF + H₂O increases at [H₂]>[F], when the flow rate of H₂ is higher than 20 sccm. Thus, the etch rate of silicon nitride has no minimum near the [F]≈[H₂] point as opposite to silicon oxide, since HF(v1) contribution to the etching is significant for silicon nitride only.

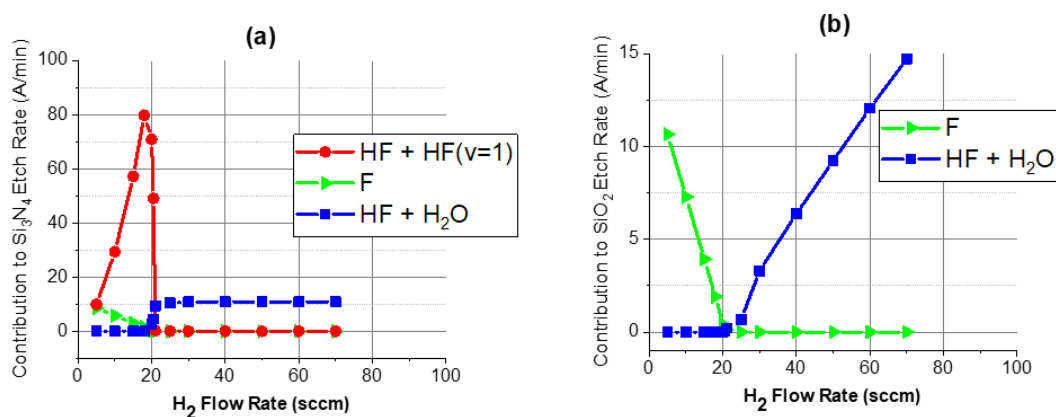


Figure 5. Contribution to the etching of: (a) Si₃N₄ and (b) SiO₂.

Section 5 is aimed to study of reactive of ion etching of silicon nitride and oxide using SF₆/H₂ and SF₆/D₂ plasmas. It was shown a kinetic isotope effect on the etching of silicon nitride only. It was used a handmade setup with CCP reactor at 40.68 MHz. Plasma interacted with the samples, the last one was located between two electrodes. Ar was injected (1 sccm) to use actinometry. H₂ and D₂ flow rates were varied from 0 to 10 sccm, other conditions were fixed: 3 sccm SF₆, 300 W, 60 mTorr.

It is shown in Fig. 6a the dependence of density of atomic fluorine on the flow rates of H₂ and D₂. The density of S₂, which is generated at relatively high level, cannot be accurately measured using actinometry, because the threshold energy of the cross section of the excitation of S₂ and Ar are significantly differ. Therefore, the intensity of B³Σ⁻_u(v0)→X³Σ⁻_u(v9) transition (283 nm) was normalized on the intensity of Ar transition (750 nm). It is assumed that I(S₂)/I(Ar) correlates with real density of S₂. The I(S₂)/I(Ar) ratio increases with hydrogen flow rates for both SF₆/H₂ and SF₆/D₂ mixtures, achieving a plateau at 6 sccm (Fig. 6b).

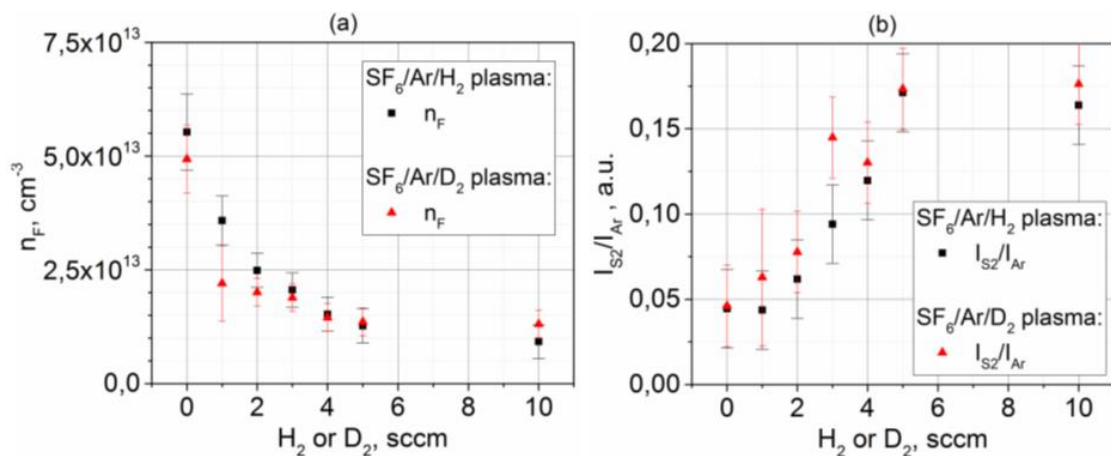


Figure 6. Dependence of the atomic fluorine density (a) and I(S₂)/I(Ar) ratio on the hydrogen flow rate (H₂ and D₂).

The dependence of the etch rate on the flow rates of hydrogen is shown in Fig. 7. According to this data the silicon nitride is etched faster even in pure SF₆ plasma. Small addition of H₂ to SF₆ discharge tends to faster etching of Si₃N₄. (the etch rate peaks at 2 sccm H₂). On the other hand, the etch rate of silicon nitride monotonically decreases with D₂ flow rate. Note that the F atom density monotonically decreases with hydrogen flow rate (Fig. 6a), therefore the etch rate peak in SF₆/H₂ plasma can be explained by the fact that vibrationally excited HF(v) molecules give contribution to the etching of silicon nitride. Note, the etch rate of Si₃N₄ monotonically with D₂ flow rate decreases in SF₆/D₂ plasma. This etch rate decline correlates with the atomic fluorine density dropping. Indeed, the vibrational quantum of DF is significantly lower than HF (0.3 eV vs 0.5 eV). Thus, it can be assumed that DF(v) has no enough energy to give visible contribution to

the etching of silicon nitride. The observed here isotope effect is not very high, because the density of atomic fluorine is very high ($\sim 10^{13} \text{ cm}^{-3}$ in Fig. 6a), therefore atomic fluorine gives the main contribution to the etching rather than vibrationally excited HF(v) molecules. Moreover, ion bombardments clean the Si_3N_4 surface from the HF molecules at the ground and vibrationally excited states.

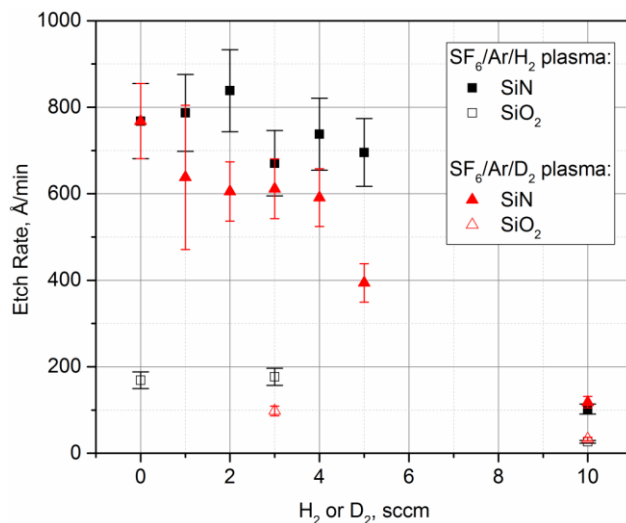


Figure 7. Dependence of Si_3N_4 and SiO_2 etch rates in SF_6/H_2 and SF_6/D_2 plasmas on hydrogen flow rate.

Section 6 is aimed to study (using integrated modelling) of mechanism precursor formation of boron nitride nanotubes growth during high temperature synthesis. First, compositions of B/N_2 mixture at thermodynamic equilibrium at various pressures and temperatures were calculated using Gibbs free energy minimization method (thermodynamic approach). Then system of kinetic equation, which describes a dissociative adsorption of N_2 molecules on small boron clusters (N_2 fixation), was numerically solved; gas cooling rate was taken into account (kinetic approach). The kinetic approach was used to check the assumption that thermodynamic equilibrium is valid during the N_2 fixation process.

The thermodynamic approach showed (Fig. 8a and 8b) that all liquid boron is consumed and converted into $\text{B}_{13}\text{N}_{12}$ chains at the temperature higher than temperature suitable for BNNT growth ($\sim 2300 \text{ K}$). The liquid boron consumption depends on pressure. Indeed, all liquid boron is consumed at $T < 2800 \text{ K}$ (1 atm) and at $T < 3600 \text{ K}$ (10 atm).

Addition of hydrogen to the reaction mixture leads to the production of HBNH iminoborane (Fig. 8c). The density of HBNH similarly changes with temperature as the density of B_mN_n chains. Thus, it can be assumed that HBNH molecule play a crucial role during the BNNT in a hydrogen contained mixtures.

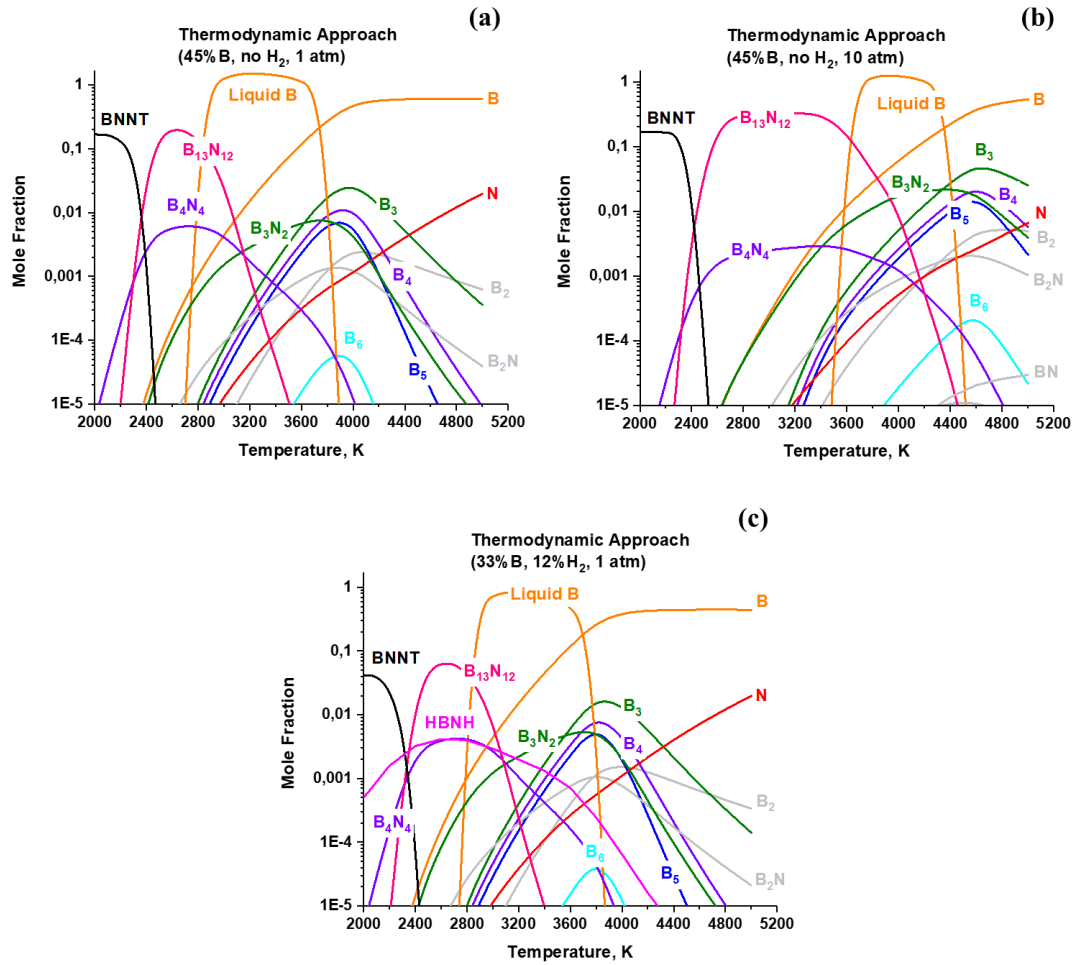


Figure 8. Composition of B/N₂ mixture at thermodynamic equilibrium at 1 atm.(a), at 10 atm.(b), for B/N₂/H₂ mixture at 1 atm.(c).

It is shown in Fig. 9 that the mole fractions of B₄N₄ and B₅N₄ significantly deviates from the equilibrium values at atmosphere pressure and higher. Thus, the kinetic approach as opposite to the thermodynamic approach showed that not all liquid boron is consumed at typical $\dot{T}_0=10^5$ K/s gas cooling rate [13] and 1 atm pressure. High pressure shifts the system towards the equilibrium, and all liquid boron is consumed at 10 atm through the reactions of dissociative adsorption of N₂ on small boron clusters (Fig. 9c).

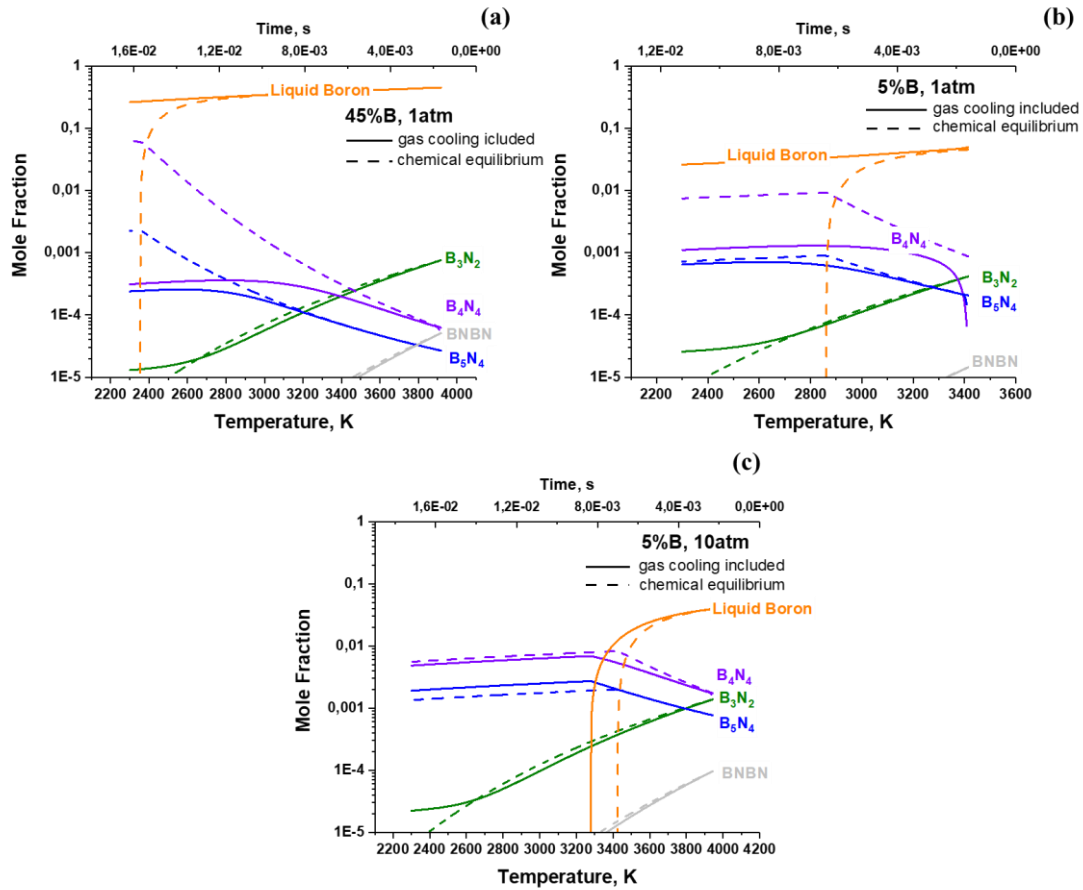


Figure 9. Results of kinetic modelling of the process of N₂ fixation at $\dot{T}_0=10^5$ K/s gas cooling rate and various conditions: 45%B and 1 atm (a), 5%B and 1 atm, 5%B and 10 atm.

Conclusion

The main goal of this research was to determine the key reagents during the highly Si₃N₄/SiO₂ selective etching. The experiments were conducted, where both Si₃N₄ and SiO₂ samples were etched by NF₃/O₂ and NF₃/O₂/N₂/H₂ plasmas. The sources of the plasmas were removed from the etched sample to exclude a damaging from UV emission and ion bombardment. Optical emission spectroscopy and mass-spectroscopy were used during the etching. The reaction mechanisms were studied using quantum chemistry methods. It was suggested analytical models, which quantitatively describe dependence of Si₃N₄ and SiO₂ etch rate on the fluxes of key reactants in NF₃/O₂ and NF₃/O₂/N₂/H₂ downstream plasmas. The densities of the key reagents were measured and calculated using plasma simulation. Thus, the Si₃N₄ etch rate curve in NF₃/O₂ mixture has a peak, where NO density peaks. The high and narrow Si₃N₄/SiO₂ selectivity peaks, which appears in NF₃/O₂/N₂/H₂, correlates with high and narrow density peak of vibration excited HF(v1) molecule.

Also, this research was aimed to study a mechanism of precursor formation of boron nitride nanotubes growth during high temperature synthesis. It was shown that boron consumption (it is the

main impediment to large scale production) occurs through the reactions of N₂ dissociative adsorption on small boron clusters (N₂ fixation) resulting in generation of B₄N₄ and B₅N₄ chains. The liquid boron is only source of the small boron clusters. A subsequent formation of longer chains occurs via collisions of B₄N₄ and B₅N₄ with each other. It was also shown that slow gas cooling rate and high pressure enhance liquid boron consumption during the synthesis, creating a good condition to large scale production of high purity and quality BNNT.

The main goal of this research was achieved. The following results can be highlighted:

1. Experimental data of highly Si₃N₄/SiO₂ selective etching by NF₃/O₂/N₂/H₂ plasma. was obtained. The Si₃N₄/SiO₂ selective is the highest among the published data (~ 380).
2. The models of NF₃/O₂ and NF₃/O₂/N₂/H₂ plasmas were developed. Calculated densities of some reagents agree with the measured densities well.
3. It was suggested the analytical models of Si₃N₄ and SiO₂ etching by remote NF₃/O₂ and NF₃/O₂/N₂/H₂ plasma sources. This models accurately reproduce measured etch rates.
4. It was shown for the first time the vibrationally excited HF(v) molecules at low density of F atoms initiate Si₃N₄ etching, while HF(v) does not affect on SiO₂ etching.
5. The detailed mechanism of N₂ fixation during high temperature synthesis was suggested.
6. It was shown for the first time, that N₂ fixation and boron consumption processes occurs at non-equilibrium regime and they depend on gas cooling rate, pressure and initial boron fraction.
7. It was shown for the first time that BN chains are the most stable compounds at the narrow temperature range. That fact complicates the synthesis of BN chains.

It can be concluded that all results are reasonable and responded to the goals of this research. The results of my research can be used to develop recipes for plasma etching in the semiconductor industry and to design a production line to large scale synthesis of boron nitride nanotubes.

It should be note that the Si₃N₄/SiO₂ selectivity by vibrationally excited HF(v) molecules can be higher than here. But it is required the additional research and experiments.

Literature

1. Tao Z. et al. FEOL dry etch process challenges of ultimate FinFET scaling and next generation device architectures beyond N3 // Proc.SPIE. 2020. Vol. 11329.
2. Lill T. Atomic Layer Processing. Willey-VCH, 2021.
3. Bassett D.W., Rotondaro A.L.P. Silica Formation during Etching of Silicon Nitride in Phosphoric Acid // Solid State Phenom. Trans Tech Publications Ltd, 2016. Vol. 255. P. 285–290.
4. Bassett D., Printz W., Furukawa T. Etching of Silicon Nitride in 3D NAND Structures // ECS Trans. 2015. Vol. 69, № 8. P. 159–167.

5. Arenal R., Lopez-Bezanilla A. Boron nitride materials: an overview from 0D to 3D (nano)structures // *WIREs Comput. Mol. Sci.* John Wiley & Sons, Ltd, 2015. Vol. 5, № 4. P. 299–309.
6. Liu Z. et al. Ultrathin high-temperature oxidation-resistant coatings of hexagonal boron nitride. // *Nat. Commun. England*, 2013. Vol. 4. P. 2541.
7. Eichler J., Lesniak C. Boron nitride (BN) and BN composites for high-temperature applications // *J. Eur. Ceram. Soc.* 2008. Vol. 28, № 5. P. 1105–1109.
8. Arenal R., Blase X., Loiseau A. Boron-nitride and boron-carbonitride nanotubes: synthesis, characterization and theory // *Adv. Phys.* Taylor & Francis, 2010. Vol. 59, № 2. P. 101–179.
9. Mirkarimi P.B., McCarty K.F., Medlin D.L. Review of advances in cubic boron nitride film synthesis // *Mater. Sci. Eng. R Reports*. 1997. Vol. 21, № 2. P. 47–100.
10. Cumings J., Zettl A. Mass-production of boron nitride double-wall nanotubes and nanococoons // *Chem. Phys. Lett.* Vol. 316. P. 211.
11. Yeh Y.-W. et al. Stable synthesis of few-layered boron nitride nanotubes by anodic arc discharge // *Sci. Rep.* 2017. Vol. 7. P. 3075.
12. Fathalizadeh A. et al. Scaled Synthesis of Boron Nitride Nanotubes, Nanoribbons, and Nanococoons Using Direct Feedstock Injection into an Extended-Pressure, Inductively-Coupled Thermal Plasma // *Nano Lett.* American Chemical Society, 2014. Vol. 14, № 8. P. 4881–4886.
13. Kim K.S. et al. Hydrogen-Catalyzed, Pilot-Scale Production of Small-Diameter Boron Nitride Nanotubes and Their Macroscopic Assemblies // *ACS Nano.* American Chemical Society, 2014. Vol. 8, № 6. P. 6211–6220.
14. Kim K.S. et al. Role of Hydrogen in High-Yield Growth of Boron Nitride Nanotubes at Atmospheric Pressure by Induction Thermal Plasma // *ACS Nano.* American Chemical Society, 2018. Vol. 12, № 1. P. 884–893.
15. Coburn J.W., Chen M. Optical emission spectroscopy of reactive plasmas: A method for correlating emission intensities to reactive particle density // *J. Appl. Phys.* American Institute of Physics, 1980. Vol. 51, № 6. P. 3134–3136.
16. Gottscho R.A., Donnelly V.M. Optical emission actinometry and spectral line shapes in rf glow discharges // *J. Appl. Phys.* American Institute of Physics, 1984. Vol. 56, № 2. P. 245–250.
17. Lieberman M.A., Lichtenberg A.J. *Principles of Plasma Discharges and Materials Processing.* John Wiley. 2005.
18. Dorai R., Kushner M.J. A model for plasma modification of polypropylene using atmospheric pressure discharges // *J. Phys. D. Appl. Phys.* 2003. Vol. 36, № 6. P. 666–685.
19. Lietz A.M., Kushner M.J. Air plasma treatment of liquid covered tissue: long timescale chemistry // *J. Phys. D. Appl. Phys.* 2016. Vol. 49, № 42. P. 425204.
20. Blain M.G., Meisenheimer T.L., Stevens J.E. Role of nitrogen in the downstream etching of silicon nitride // *J. Vac. Sci. Technol. A.* American Vacuum Society, 1996. Vol. 14, № 4. P. 2151–2157.
21. Blain M.G. Mechanism of nitrogen removal from silicon nitride by nitric oxide // *J. Vac.*

- Sci. Technol. A. American Vacuum Society, 1999. Vol. 17, № 2. P. 665–667.
22. Habuka H., Otsuka T. Reaction of Hydrogen Fluoride Gas at High Temperatures with Silicon Oxide Film and Silicon Surface // Jpn. J. Appl. Phys. IOP Publishing, 1998. Vol. 37, № Part 1, No. 11. P. 6123–6127.
 23. Kang J.K., Musgrave C.B. The mechanism of HF/H₂O chemical etching of SiO₂ // J. Chem. Phys. 2002. Vol. 116, № 1. P. 275–280.
 24. Cramer J.C. Essentials of Computational Chemistry. airy Science & Technology, CRC Taylor & Francis Group, 2014. 1–542 p.
 25. Eyring H. The Activated Complex in Chemical Reactions // J. Chem. Phys. 1935. Vol. 3, № 2. P. 107–115.
 26. Frisch M.J. et al. Gaussian, Inc., Wallingford CT: Revision E.01. 2016.